Biological Psychiatry: CNNI

Archival Report

Data-Driven Clustering Reveals a Link Between Symptoms and Functional Brain Connectivity in Depression

Luigi A. Maglanoc, Nils Inge Landrø, Rune Jonassen, Tobias Kaufmann, Aldo Córdova-Palomera, Eva Hilland, and Lars T. Westlye

ABSTRACT

BACKGROUND: Depression is a complex disorder with large interindividual variability in symptom profiles that often occur alongside symptoms of other psychiatric domains, such as anxiety. A dimensional and symptom-based approach may help refine the characterization of depressive and anxiety disorders and thus aid in establishing robust biomarkers. We use resting-state functional magnetic resonance imaging to assess the brain functional connectivity correlates of a symptom-based clustering of individuals.

METHODS: We assessed symptoms using the Beck Depression and Beck Anxiety Inventories in individuals with or without a history of depression (N = 1084) and high-dimensional data clustering to form subgroups based on symptom profiles. We compared dynamic and static functional connectivity between subgroups in a subset of the total sample (n = 252).

RESULTS: We identified five subgroups with distinct symptom profiles, which cut across diagnostic boundaries with different total severity, symptom patterns, and centrality. For instance, inability to relax, fear of the worst, and feelings of guilt were among the most severe symptoms in subgroups 1, 2, and 3, respectively. The distribution of individuals was 32%, 25%, 22%, 10%, and 11% in subgroups 1 to 5, respectively. These subgroups showed evidence of differential static brain-connectivity patterns, in particular comprising a frontotemporal network. In contrast, we found no significant associations with clinical sum scores, dynamic functional connectivity, or global connectivity.

CONCLUSIONS: Adding to the pursuit of individual-based treatment, subtyping based on a dimensional conceptualization and unique constellations of anxiety and depression symptoms is supported by distinct patterns of static functional connectivity in the brain.

Keywords: Anxiety, Depression, fMRI, Functional connectivity, Heterogeneity, Symptom-based clustering

https://doi.org/10.1016/j.bpsc.2018.05.005

Major depressive disorder is among the leading contributors to years lived with disability (1) and is the leading cause in 56 countries (2,3). Although several brain regions, including the subgenual anterior cingulate (4), have been implicated in the pathophysiology of depression, global efforts in identifying sensitive, specific, and clinically predictive brain correlates of mood disorders have not yet succeeded (5,6). One reason for the lack of robust imaging-based characteristics is that depression is a heterogeneous construct in terms of symptom constellation. For example, based on 12 items from the Quick Inventory of Depressive Symptomatology, Fried and Nesse (7) found evidence of 1030 unique symptom profiles among 3703 outpatients with depression. Furthermore, depression and anxiety symptoms often co-occur; for example, 75% of individuals with a depressive disorder in the Netherlands Study of Depression and Anxiety also fulfilled the criteria for an anxiety disorder (8). Adding to the complexity, individuals in the general, healthy population from time to time also experience subclinical symptoms of depression and anxiety at various degrees.

Methodological variability is another reason for the mixed brain-imaging findings in depression, especially for functional magnetic resonance imaging (fMRI)–based measures of brain activation (6) and connectivity (9). The functions of a healthy mind are supported by the continuous cross talk between different brain regions (10). Dysregulations in this fine-tuned and complex interplay may increase susceptibility for mental disorders (11). Supporting the conceptualization of depression as a network-based disorder, fMRI-based functional connectivity (FC) studies have implicated large-scale brain-network dysfunction in depression (9). Whereas previous studies have reported results primarily from various estimates of static FC (sFC), the temporal correlation between two brain regions across the entire time series, there is an increasing awareness of the relevance of dynamic FC (dFC), the variability in the temporal correlations across the

 ISSN: 2451-9022

time series (12,13). Interestingly, sFC and dFC capture distinct properties of brain-network dynamics (14,15) and may therefore provide complementary information in depression (16).

Here, to address symptom heterogeneity in depression and related subclinical phenotypes, we used high-dimensional data-driven clustering (HDDC) (17) based on item scores on the Beck Depression Inventory II (BDI-II) and Beck Anxiety Inventory (BAI) to identify groups of individuals with distinct symptom profiles among 1084 individuals with or without a history of a diagnosis of depression. To assess the brain-system-level relevance of the symptom-based subgroups, we used network-based statistics (NBS) to compare measures of resting-state fMRI–based static and dynamic FC between groups in a subset of 252 individuals.

METHODS AND MATERIALS

Sample

In the total sample (N = 1084), 605 individuals with a history of major depressive episodes (MDEs) and 437 individuals with no history of an MDE were included (Table 1). Participants were drawn from four research projects at the Clinical Neuroscience Research Group, Department of Psychology, University of Oslo (see the Supplemental Methods and Materials). A subsample of 252 participants (Table 2) who were drawn from one of these research projects (see the Supplemental Methods and Materials) was assembled for an MRI substudy. In the total sample, individuals with a history of depression were diagnosed using the Structural Interview for DSM-IV (18) in one of the substudies and Mini International Neuropsychiatric Interview 6.0 (19) in the other three, and they were recruited mainly from outpatient clinics. Individuals with no history of depression had been recruited by posters, advertisements in the local newspaper, and social media. The number of lifetime MDEs and history of anxiety, mania or hypomania, and other major Axis I psychiatric disorders were assessed for all individuals based on either the Mini International Neuropsychiatric Interview 6.0 or Structural Interview for DSM-IV. Current selective serotonin reuptake inhibitor use was evaluated through a semi-structured interview. Individuals with a history of neurological disorders or MRI contraindications (for the MRI sample) were excluded. The study was approved by the Regional Ethical Committee of South-Eastern Norway, and all participants provided informed consent prior to enrollment.

Clinical Inventories

All participants completed the BDI-II (20) and BAI (21), comprising 21 items assessing current symptoms, during recruitment and within 1 to 2 weeks of the MRI sessions (for the MRI subsample). The originally proposed somatic-affective subscales (12 items each for BDI-II and BAI) and cognitive factor subscales (9 items each for BDI-II and BAI) were used in further analyses. Summary statistics for each item by group are shown in Supplemental Table S1, and a correlation plot with a dendrogram based on hierarchical clustering across all items is shown in Supplemental Figure S1. Largest scores across groups were observed for loss of energy (BDI15), changes in sleeping pattern (BDI16), tiredness or fatigue (BDI20), nervous (BAI10), and indigestion (BAI18). The distribution of BDI-II and BAI sum scores by group are shown in Supplemental Figure S2.

Table 1. Demographics for the Total Sample

	Individuals With No History of Depression (n = 437)	Individuals With a History of Depression[a] (n = 605)	p[b]
Gender[c], Female (%)	287 (66)	468 (77)	<.001
Age[d], Years, Mean (SD)	33.9 (13.4)	39.5 (12.9)	<.001
Depression Symptoms			
BDI-II, mean (SD)	4.5 (5.5)	14.1 (11.2)	<.001
Anxiety Symptoms			
BAI, mean (SD)	3.2 (4.1)	8.7 (8.4)	<.001
Other			
History of anxiety disorder, n	7	153	<.001
History of mania or hypomania, n	0	53	<.001
History of other Axis I disorders, n	2	45	<.001
Number of depressive episodes[e], mean (SD)	0	4.1 (6.5)	<.001
Currently medicated (SSRI)[f], n	0	164	<.001

BAI, Beck Anxiety Inventory; BDI-II, Beck Depression Inventory II; SSRI, selective serotonin reuptake inhibitor.

[a]An additional 42 cases were left out of the table because the extent of the depressive episode could not be determined from the records. However, these cases were included in the symptom-based clustering.

[b]p denotes the p value from group comparisons using χ^2 tests for gender, history of additional disorders, and current SSRI medication status, while we used Mann-Whitney U tests for the rest.

[c]For gender, data for 2 cases were missing.

[d]For age, data for 25 cases were missing.

[e]For the number of major depressive episodes, data for 36 cases were missing.

[f]The current SSRI status of 57 participants in the patient group was not recorded.

Table 2. Demographics of the Magnetic Resonance Imaging Subsample

	Individuals With No History of Depression (n = 72)	Individuals With a History of Depression[a] (n = 178)	p[b]
Gender, Female, n (%)	48 (67)	127 (71)	.389
Age, Years, Mean (SD)	42.5 (13.6)	38.9 (13.4)	.099
Education Level (ISCED)[c], Mean (SD)	6.0 (1.0)	5.9 (1.2)	.757
Depression Symptoms			
HAM-D[d], mean (SD)	2.9 (2.1)	8.0 (5.8)	<.001
BDI-II, mean (SD)	1.6 (2.9)	11.8 (10.4)	<.001
Anxiety Symptoms			
BAI, mean (SD)	1.7 (2.8)	8.2 (8.1)	<.001
Other			
AUDIT[e], mean (SD)	4.8 (3.3)	6.3 (5.2)	0.139
DUDIT[f], mean (SD)	0.5 (1.9)	0.9 (2.7)	0.106
Left-handedness, n	7	6	
History of anxiety disorder, n	1	53	<.001
History of mania or hypomania, n	0	30	
History of other Axis I disorders, n	0	24	<.001
Number of depressive episodes, mean (SD)	0	4.3 (5.8)	<.001
Currently medicated (SSRI), n	0	55	<.001

AUDIT, Alcohol Use Disorders Identification Test; BAI, Beck Anxiety Inventory; BDI-II, Beck Depression Inventory II; DUDIT, Drug Use Disorders Identification Test; HAM-D, Hamilton Depression Rating Scale; ISCED, International Standard Classification of Education; SSRI, selective serotonin reuptake inhibitor.

[a]2 cases not reported here have generalized anxiety disorder and an uncertain history of major depressive episodes but are used in the magnetic resonance imaging analysis.

[b]p denotes the p value from group comparisons using χ^2 tests for gender, handedness, history of additional disorders, and current SSRI medication status, while we used Mann-Whitney U tests for the rest.

[c]6 cases were missing information about ISCED level.

[d]4 cases were missing HAM-D scores.

[e]4 cases were missing AUDIT scores.

[f]5 cases were missing DUDIT scores.

High-Dimensional Data-Driven Clustering

BDI-II and BAI symptom scores were Z-normalized and submitted to HDDC in the R package HDclassif (22). HDDC is an unsupervised clustering method based on the Gaussian mixture model, and it has been shown to outperform similar methods in the R package mclust (23) in terms of accuracy (22). We chose the default and most general model of HDDC, which entails both free variances and dimensions across clusters, as well as cluster-specific noise and cluster-specific orientation matrix. HDDC also calculates the probability of each subject's belonging to each of the clusters, which was used in subsequent analyses. We established the optimal number of clusters using the Bayesian information criterion (22) and performed various analyses to assess the robustness and stability of the clustering (see the Supplemental Results) using the clusteval R package (24). To characterize the symptom profiles of each subgroup, we focused on the symptoms that are most severe. Further, based on the partial correlation matrix, we assessed the eigenvector centrality of each symptom using the eigenvector_centrality_und.m function in the Brain Connectivity Toolbox (25) in MATLAB R2016b (The MathWorks, Inc., Natick, MA), yielding a graph-based metric reflecting symptom centrality or importance. Additional centrality measures, strength, betweenness, and closeness were computed using the R package qgraph (26) (see the Supplemental Methods and Materials).

Image Acquisition

MRI was performed on a 3T Philips Ingenia scanner (Philips Medical Systems, Best, Netherlands) at the Oslo University Hospital using a 32-channel head coil. The details of the full imaging protocol, including fMRI and T1-weighted sequences, are in the Supplemental Methods and Materials. Because of the technical specifics of the MRI acquisition protocol (see the Supplemental Methods and Materials), phase-encoding direction was included as a factor in all relevant analyses.

Image Processing

FEAT from the FMRIB Software Library (27) was used for fMRI data processing. This involved brain extraction, motion correction (MCFLIRT) (28), spatial smoothing (Gaussian kernel, full width at a half maximum width of 6 mm), high-pass filtering (100 seconds), and single-session independent component analysis (ICA) (MELODIC). Estimated mean relative in-scanner head motion (volume-to-volume displacement) was computed with FSL's MCFLIRT. FMRIB'S ICA-based Xnoiseifier (FIX) (29,30) was used to automatically classify noise components and regress them from the main signal, with a threshold of 60. FIX has been shown to substantially improve the temporal signal-to-noise ratio (31,32), which was computed before and after FIX (33). In line with the findings of previous studies (31,32,34), denoising substantially increased temporal

signal-to-noise ratio (t = 36.177, $p < .001$, Cohen's d = 1.86), and none of the scans were deemed to have insufficient quality after denoising.

T1-weighted volumes were skull-stripped using FreeSurfer 5.3 (35) and used for standard space (MNI152) registration with FLIRT, refining the process with boundary-based registration (36) and FNIRT.

Group ICA on fMRI Data

To avoid bias due to unequal group sizes, group-level ICA was performed on a balanced subset of individuals with a history of depression and individuals with no history of depression (n = 72 from each group) (37). Model order was fixed at 40, which provides a reasonable trade-off between anatomical sensitivity and specificity (38). Independent component spatial maps and corresponding time series were estimated using dual regression (39). We assessed the spatial maps and frequency profiles, following previous recommendations (40). We identified and regressed out the time series of 15 noise components, and an additional 6 components (see Supplemental Figure S3) were discarded from further analyses since their spatial maps did not conform with any established resting-state networks or were a mixture between signal and noise, leaving 19 independent components for connectivity analyses.

Local FC: sFC and dFC

For sFC, a node-by-node connectivity matrix was created using partial correlations between the time series, resulting in 171 unique edges. These partial correlations were L1-regularized, with estimated regularization strength (lambda) at the subject level (37,41,42).

For dFC we used a phase-based method in line with a recent application in aging and dementia (34). Here, the degree of coupling and decoupling between pairs of brain nodes is conceptualized as the coefficient of variation of delta phi, which is the normalized differences in their wave phases. First, each of the 19-node time series was narrow-band filtered within 0.04 to 0.07 Hz, which is required to obtain meaningful phases (43). Next, we applied the Hilbert transform, creating an analytic signal, in which we computed the instantaneous phase values for each of the 19 independent components. Last, we estimated the Kuramoto order, an index of oscillation between regions at every instant (44).

Global-Brain-Level FC

For each individual sFC connectome, we calculated global efficiency, a graph-based measure of topological organization defined as the average inverse shortest path length in a network, using the efficiency_wei.m function in the Brain Connectivity Toolbox (25). This is described in detail in the study by Rubinov and Sporns (25). Metastability, a measure of dynamic flexibility whereby the brain transitions through different states, was computed as the standard deviation of the Kuramoto order parameter (45,46). Higher metastability is a potential marker for cognitive and behavioral functioning (45,47–49). Synchrony, a measure of general coherence (50), was computed as the mean of the Kuramoto order parameter. It is hypothesized that such coherence allows for the exchange of information within the brain (51). See the studies by Córdova-Palomera *et al.* (34) and Váša *et al.* (50) for a detailed description of synchrony and metastability.

Statistical Analyses

Differences between subgroups in between-node (edgewise) sFC and dFC were tested by means of analysis of covariance including subgroup, gender, age, phase-encoding direction, and mean relative motion. We used the same approach to test for differences in diagnosis between individuals with a history of depression and individuals with no history of depression. For inference, we used NBS (52) (10,000 permutations, α = .05), in which an initial uncorrected threshold at the edge level is chosen. Then, the familywise error rate is controlled by measuring the clustering structure of the edges that survive the initial threshold. Here, we tested for the main effects of a subgroup and the probability of belonging to a specific subgroup on FC. To assess the relative importance of each node, we computed the sum of the test statistic across all edges. We used a similar approach to test for associations between the BDI-II and BAI sum and subscale scores with FC.

We used analysis of covariance in R (53) to independently test for association between subgroup and global efficiency, and metastability and synchrony, respectively, controlling for gender, age, phase-encoding direction, and mean relative motion. We used the same model to assess the association between the BDI-II and BAI sum and subscale scores with global efficiency, metastability, and synchrony independently.

We used Kruskal-Wallis rank-sum tests and χ^2 tests to assess subgroup differences in key demographic and clinical variables. We used Kolmogorov-Smirnov tests to assess the similarity of the subgroups from the total sample and MRI subsample based on key clinical and demographic characteristics.

RESULTS

Individual Clustering Using HDDC

HDDC yielded five symptom-based subgroups with differing symptom profiles. In terms of the distribution, 342 (32%), 272 (25%), 240 (22%), 106 (10%), and 124 (11%) of the participants from the total sample were in subgroups 1 to 5, respectively. Figure 1 shows the mean scores of each symptom for each of the subgroups and the sum scores for the BDI-II and BAI, while Supplemental Figure S4 shows the BDI-II and BAI subscale sum scores. Overall, the subgroups seemed to differ by total severity. However, several other patterns should be noted, in terms of which symptoms are most severe in the subgroups and especially eigenvector centrality (Figure 2). Unable to relax (BAI4) was among the most severe symptoms in subgroup 1. Feelings of dislike (BDI7), worthlessness (BDI14), and loss in interest (BDI12) showed highest eigenvector centrality in subgroup 1, with low eigenvector centrality for the BAI symptoms. Fear of worst happening (BAI5) was among the most severe in subgroup 2. Sadness (BDI1), feelings of guilt (BDI5), and tiredness or fatigue (BDI20) showed highest eigenvector centrality in subgroup 2, and the eigenvector centrality was higher across BAI symptoms. Feelings of guilt (BDI5) was more severe in subgroup 3. Tiredness or

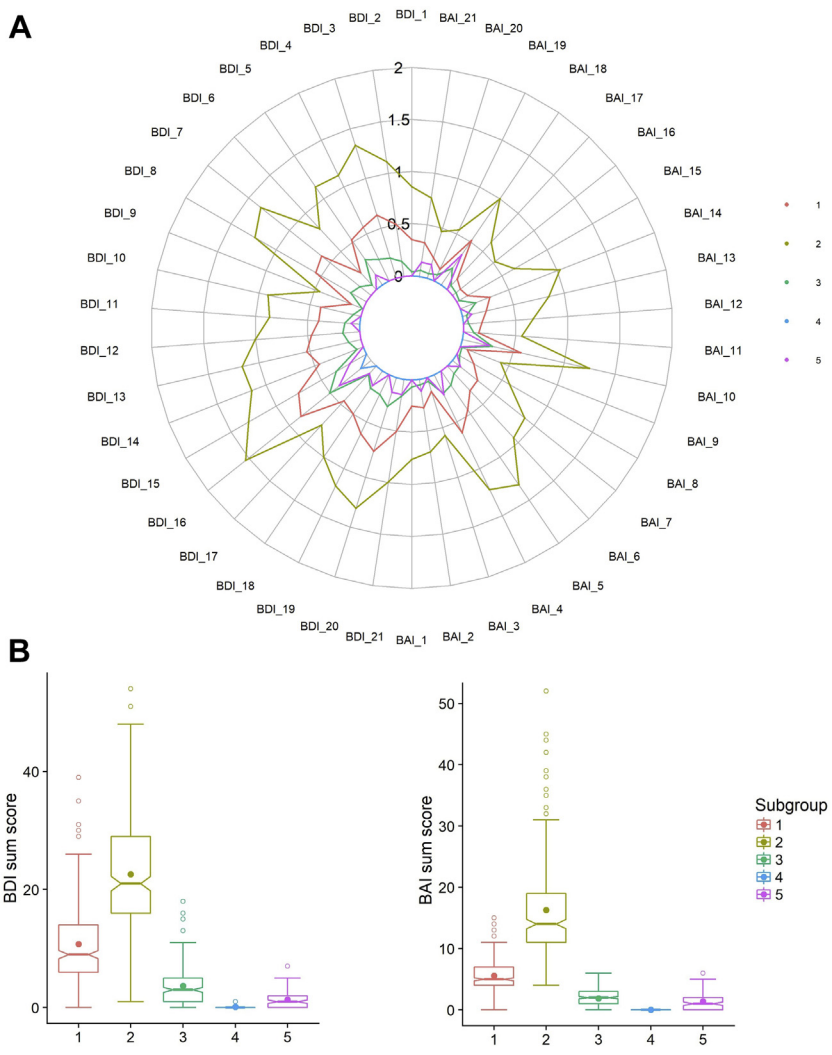

Figure 1. Symptom profiles of the subgroups from high-dimensional data-driven clustering. **(A)** Mean symptom score of each item of each subgroup. **(B)** Box plots of total (left) Beck Depression Inventory (BDI) and (right) Beck Anxiety Inventory (BAI) scores for each subgroup.

fatigue (BDI20), loss of energy (BDI15), and loss of pleasure (BDI4) showed high eigenvector centrality in subgroup 3. Notably, although the overall symptom severity in subgroup 5 was lower than that in subgroup 3, several symptoms were more severe in subgroup 5, and there was an absence of 27 of the total 42 symptoms. Across all subgroups, changes in sleeping pattern (BDI16) was among the most severe, and it was the only symptom present in subgroup 4. Distinct subgroup differences were seen in strength, closeness, and betweenness centrality (Supplemental Figure S5), which were similar to the eigenvector centrality results.

We did not compute centrality measures for subgroups 4 and 5, as these were characterized by a lack of many symptoms and would not be comparable to the other subgroups as centrality measures for a given symptom are dependent on the whole network. The Spearman correlation between mean symptom score and eigenvector centrality for subgroups 1, 2, and 3 yields ρ values of .627 ($p < .001$), .683 ($p < .001$), and .506 ($p < .001$), respectively.

Healthy control subjects and patients were present in all subgroups (Supplemental Figure S6), yet the proportion of patients was higher in subgroups with the highest severity scores, specifically subgroups 2 and 1 ($\chi^2 = 109.69$, $df = 4$, $p < .001$). Key demographic and clinical characteristics of the subgroups for the MRI subsample and total sample are shown in Table 3 and Supplemental Table S2, respectively. There are no differences in the key demographic variables, such as age and gender, or MRI quality metrics, but there are differences in several of the clinical features, including history of anxiety disorders. The stability analyses suggest that the clusters were robust, with ~0.75 Jaccard index being the most common for every pair of iterations (Supplemental Figures S7 and S8).

The mean scores of each symptom for each of the MRI-subsample subgroups (Supplemental Figure S9) are very similar to the symptom profiles of the total sample subgroups. Kolmogorov-Smirnov tests revealed no significant differences between the total sample subgroups or MRI-subsample

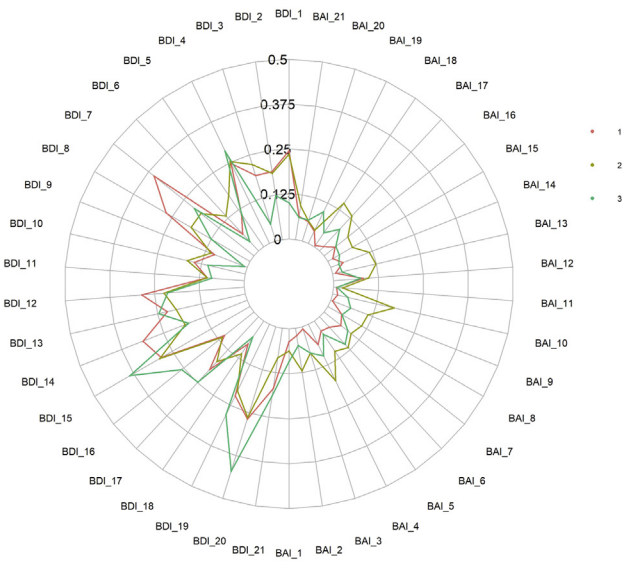

Figure 2. Eigenvector centrality of symptoms for subgroups 1, 2, and 3. Subgroup 4 could not be included because only one symptom, changes in sleeping pattern, was present. Subgroup 5 was excluded because of the absence of many symptoms (27 of 42), which would change the underlying centrality weighting. BAI, Beck Anxiety Inventory; BDI, Beck Depression Inventory.

subgroups on all clinical and demographic variables, except for the number of MDEs (Supplemental Table S3).

fMRI-Based Static FC

NBS revealed a 22-edge subnetwork with significant main effect of subgroup (p = .033, corrected using permutation testing) (Figure 3A). The uncorrected edge-level test statistics for this subnetwork are shown in Supplemental Table S4. The strongest differences were seen in edges connecting a default mode network (DMN) component and the frontotemporal network (IC5–IC16) and between the precuneus and the frontotemporal network (IC7–IC16) (Figure 3B). Figure 3C shows the sum of the test statistics of each node, with the largest cumulative effects seen in two DMN components (IC5 and IC6), precuneus (IC7), frontotemporal network (IC16), cerebellum (IC31), and thalamus (IC39).

NBS revealed a 30-edge subnetwork with significant association with the probability of belonging to subgroup 1 (p = .015) (Figure 4A) and a 24-edge subnetwork with significant association with the probability of belonging to subgroup 3 (p = .042) (Figure 4A). Figure 4B shows the nodes with the largest cumulative effect on the statistical significance of these two subnetworks.

We found no significant associations between diagnosis and sFC, or BDI-II and BAI sum or subscale scores and sFC (Supplemental Table S5).

Dynamic FC

NBS revealed no significant main effect of subgroup or diagnosis on dFC. We found no significant association of BDI-II and BAI sum or subscale scores with dFC (Supplemental Table S6).

Global-Brain-Level Analyses

There was no significant association of diagnosis, subgroup, or BDI-II and BAI sum or subscale scores with global efficiency, synchrony, or metastability (Supplemental Table S5).

DISCUSSION

Using high-dimensional clustering of individuals based on current symptoms of depression and anxiety, we have identified five subgroups cutting across diagnostic boundaries in 1083 participants with a history or no history of depression. Furthermore, individuals with and without a history of depression were present in all subgroups. Subsequent analysis in an MRI subsample revealed a brain sFC pattern with main effect of subgroup, with the frontotemporal network as a major node. There were no significant associations with diagnosis or conventional symptom domains, supporting the idea that data-driven clustering provides a more biologically sensitive grouping.

Table 3. Key Clinical and Demographic Factors of the Subgroups for the Magnetic Resonance Imaging Subsample

	Subgroup 1 (n = 66)	Subgroup 2 (n = 68)	Subgroup 3 (n = 58)	Subgroup 4 (n = 34)	Subgroup 5 (n = 25)	p^a
Individuals With a History of Depression, n (%)	59 (89)	66 (97)	37 (64)	11 (32)	5 (2)	<.001
Gender, Female, n (%)	42 (64)	51 (75)	36 (62)	28 (82)	18 (72)	.178
Age, Years, Mean (SD)	39.0 (12.2)	38.2 (14.7)	39.6 (13.0)	44.5 (13.1)	40.3 (14.6)	.273
History of Anxiety Disorder, n (%)	15 (23)	28 (42)	9 (16)	2 (6)	1 (4)	<.001
History of Mania or Hypomania, n (%)	7 (11)	12 (18)	2 (3)	3 (9)	1 (4)	.081
History of Other Axis I Disorders, n (%)	8 (12)	13 (19)	0 (0)	3 (9)	0 (0)	.002
Number of MDEs, Mean (SD)	4.6 (5.7)	4.5 (7.4)	2.1 (2.8)	0.8 (1.2)	0.72 (1.4)	<.001
Currently Medicated (SSRI), n (%)	15 (23)	23 (34)	10 (17)	5 (15)	2 (8)	.036
Head Motion, Mean (SD)	0.082 (0.040)	0.083 (0.043)	0.087 (0.043)	0.081 (0.036)	0.085 (0.038)	.819
tSNR Before FIX, Mean (SD)	154.05 (31.04)	159.17 (27.34)	152.13 (27.17)	156.44 (23.89)	151.15 (31.27)	.384
tSNR After FIX, Mean (SD)	219.22 (41.00)	227.50 (43.74)	216.64 (36.22)	214.05 (31.11)	206.68 (38.98)	.235

MDE, major depressive episode; SSRI, selective serotonin reuptake inhibitor, tSNR, temporal signal-to-noise ratio.
[a]p denotes the p value assessing the main effect of subgroup using χ^2 tests for gender, history of disorders, and current SSRI medication status, while we used Kruskal-Wallis rank-sum tests for the rest.

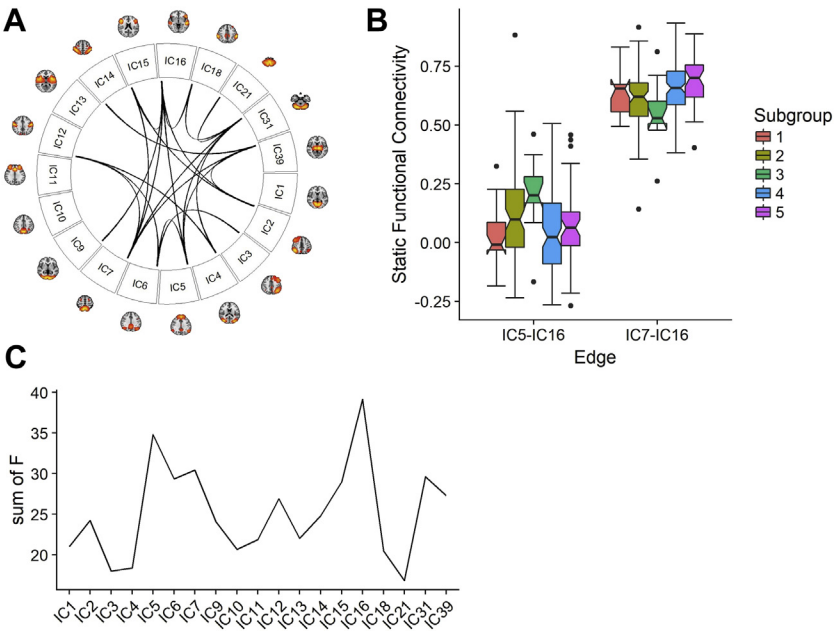

Figure 3. Results from the main effect of subgroup on static functional connectivity using network-based statistics. **(A)** A circular plot showing the 21-edge subnetwork. **(B)** A box plot of the raw static functional connectivity values of the two edges that show the largest main effect of subgroup; between a default mode network component and the frontotemporal network, and between the precuneus and the frontotemporal network. **(C)** Sum of test statistic (*F*) showing the cumulative effect of an independent component (IC) node on the subgroup main effect.

Previous studies have used similar methods to provide data-driven symptom-based stratifications of depression. Several studies have identified a melancholic and a separate atypical subgroup (54–56), which is in line with the DSM-V definition (57). The most common pattern across such studies is total severity difference (58), which provides support for a dimensional symptom-based approach. Despite this, the subgroups in the current study exhibit unique symptom profiles in the pattern of individual symptom severity and especially in centrality. Notably, subgroup 5 has an absence of many symptoms, while the only symptom in subgroup 4 was changes in sleeping pattern, showing a high degree of specificity. Interestingly, at least one of the three main symptoms that must be present for an MDE in the DSM-V has different eigenvector centralities in the subgroups: sadness and loss in interest have higher centrality in subgroup 1, whereas loss of pleasure has higher eigenvector centrality in subgroup 3. Additionally, subgroup 3 is distinct in that tiredness or fatigue

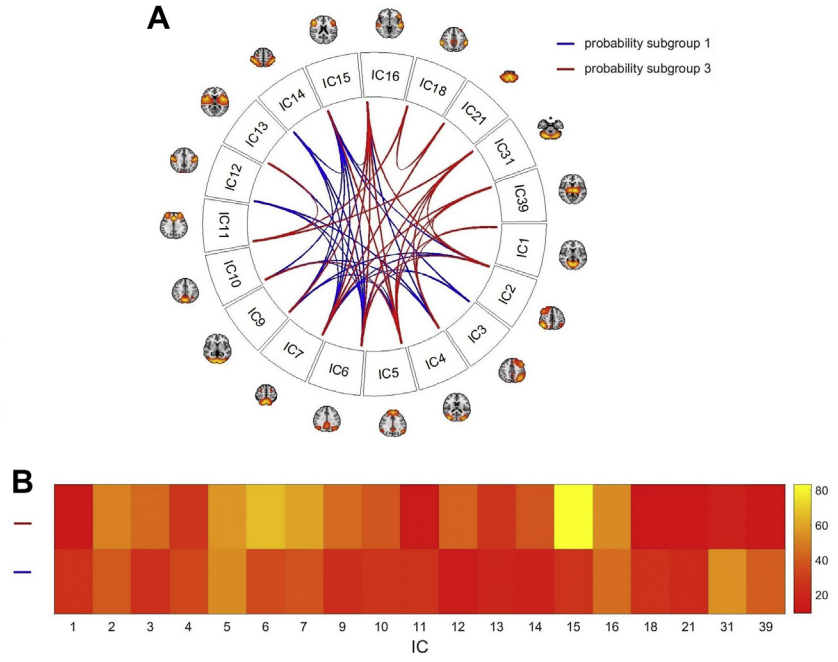

Figure 4. Results from the static functional connectivity association with the probability of belonging to specific subgroups. **(A)** Static functional connectivity association with the probability of belonging to subgroup 1 (blue) and subgroup 3 (red). **(B)** Sum of test statistic (*F*) showing the cumulative effect of an independent component (IC) node with the association of the probability of belonging to subgroup 1 (upper row) and subgroup 3 (bottom row).

and loss of energy seem to have much higher eigenvector centrality than in the other subgroups. Intriguingly, there was a distribution of individuals with and without a history of depression across all subgroups in the current study. This likely explains the differences in clinical features across subgroups, as most of the individuals with no history of depression have an absence of any history of psychiatric diagnosis, with only a few exceptions for anxiety. It is interesting that individuals with these various clinical characteristics are present across all subgroups despite the overall differences.

Data-driven subtyping may have clinical relevance. In a 2-year follow-up study (59), the group with persistent depression had higher centrality in fatigue or loss of energy at baseline compared with that of the remitted group. This symptom specificity could suggest that such subgroups have different underlying mechanisms and environmental triggers. For instance, life stress has been shown to have a substantial impact on interest (60), whereas romantic breakup was strongly associated with guilt (61). Changes in sleeping pattern is the most severe symptom across all the subgroups, implying that it is more prominent than expected in terms of traditional diagnostic criteria. Recently, different sleep profiles were independently associated with specific patterns of depression comorbidity (62) and distinct abnormalities in DMN functioning (63).

The subgroups showed differential sFC in a range of brain networks, especially those involving the frontotemporal node (IC16). The brain regions encompassing this node are involved with executive functions (64,65) and external information processing (66). Two DMN subcomponents (IC5 and IC6) were among the nodes that contributed the most to the network, which can indicate negative self-referential processes (67,68). Another such node was the precuneus (IC7), where activity within has been associated with increased number of depressive episode (69) and rumination (70). Two other implicated nodes were the cerebellum (IC31) and the thalamus (IC39). Lower cerebellar volume has been associated with decreased emotional memory (71), whereas thalamic volume reduction has been associated with deficits in top-down regulation of negative emotions in depression (72). Intriguingly, we observed unique sFC patterns associated with the probability of belonging to subgroups 1 and 3, with only a 5-edge overlap. Here, subgroup 3 was uniquely associated with sFC in the supramarginal (IC18), motor (IC21), cerebellar (IC31), and thalamic (IC39) nodes, while subgroup 1 was associated with a higher cumulative effect of the inferior-midfrontal node (IC15).

We found no differences in dFC, global efficiency, metastability, or synchrony between the subgroups. We found no significant association between diagnosis or any of the symptom scores with any of the FC measures. Taking these findings together, the sFC associations with the subgroups are partly explained by the specificity of symptom profiles beyond total severity differences. Therefore, we argue that a symptom-based rather than a syndrome-based approach is better suited for elucidating depression symptom heterogeneity.

Two recent studies have identified biotypes of depression, based on sFC. Drysdale *et al.* (73) identified four biotypes, whereby biotypes 1 and 2 are similar to subgroup 3 in terms of fatigue, biotype 3 is similar to subgroup 1 in terms of interest, and biotype 4 is similar to subgroup 2 in that anxiety is prominent. The most important features in these biotypes were frontostriatal network dysfunction coupled with anhedonia, and limbic network dysfunction coupled with anxiety. Intriguingly, these subgroups responded differentially to an experimental transcranial magnetic stimulation treatment, showing the potential clinical utility of such subgrouping. The other study (74) identified one biotype characterized by typical DMN connectivity and a second biotype with increased dorsal anterior cingulate connectivity with higher rates of anxiety; the study consisted predominantly of female subjects. The difference in rates of anxiety is similar to the finding in the current study. Both previous studies and the current study highlight the importance of anxiety in depression, suggesting that there is some convergence across FC and symptom-based clustering. However, FC-based clustering methods are novel, needing validation and replication in independent studies. A strength of the current study is a more detailed range of symptoms.

One limitation of this study is that we included few severely depressed patients, which may have biased the results toward the less severe end of the spectrum. The subgroups from the total sample and MRI subsample were very similar on all other key clinical and demographic characteristics, except for the number of depressive episodes. This could be due to differences in the assessment procedure. Regardless, a recent large-scale meta-analysis of depression studies (6) found no differences in fMRI results when accounting for several clinical characteristics, including medication and comorbidity.

Another limitation is the extent to which BDI-II and BAI capture the spectrum of depression and anxiety symptoms. For instance, they assess only typical patterns (e.g., decreased appetite, insomnia) rather than atypical symptoms (e.g., hypersomnia, increased appetite). However, there is some debate as to what exactly constitutes depression symptoms (75,76), as evidenced by the lack of overlap among several depression scales (77). Although changes in sleeping pattern was among the most severe symptom across all subgroups, this is not uniquely associated with depression and could be due to somatic comorbidity.

Considering that NBS allows for clusterwise inference, caution is warranted when interpreting single edges that constitute a cluster in its entirety, in particular when it is applied on a multigroup factorial design, as was done here. Methodological variability may account for the discrepancy in previous fMRI findings (16,78,79)—for example, those related to the definition of the nodes (e.g., ICA-based vs. region of interest–based) and edges (e.g., full vs. partial correlations). Based on graph-theoretical accuracy, ICA has been shown to outperform region of interest–based node definition, and regions of interest may not conform well with functional and anatomical boundaries (80,81). Sliding-window analyses are the most common method of analyzing dFC, but one issue is unsuitability for fMRI sequences that are $<$10 minutes (82). Head motion is a major confounder in FC studies (83,84), but this was taken into account in the analyses.

Conclusions

We identified five robust subgroups with specific clinical symptom profiles. fMRI analysis revealed that these subgroups

were characterized by distinct static brain-connectivity patterns, in particular implicating a frontotemporal node. These neurobiologically sensitive subgroups based on a dimensional and symptom-based approach may help move the field toward precision and individualized treatment of depression.

ACKNOWLEDGMENTS AND DISCLOSURES

This work was supported by the South-Eastern Norway Regional Health Authority (Grant Nos. 2014097 [to LTW], 2015073 [to LTW], and 2015052 [to NIL]), the Research Council of Norway (Grant Nos. 249795 [to LTW], 229135 [to NIL], and 175387/V50 [to NIL]), and the Department of Psychology, University of Oslo (LAM).

LAM, NIL, and LTW designed this study. LAM, RJ, and EH collected both the clinical and MRI data. LAM performed the statistical analyses with major input from TK, AC-P, and LTW. LAM wrote the manuscript and interpreted the results with major input from NIL and LTW as well as from all other authors.

We thank Ragnhild Bø and Martin Aker for providing clinical data from their respective research projects. We thank Grethe Løvland and Svein Are Vatnehol for assistance with the technical aspects of the MRI protocol. Finally, we thank Dani Beck for substantial contribution of the MRI data acquisition.

NIL has previously received consultancy fees and travel expenses from Lundbeck. All other authors report no biomedical financial interests or potential conflicts of interest.

ARTICLE INFORMATION

From the Clinical Neuroscience Research Group (LAM, NIL, RJ, EH), Department of Psychology (LTW); Norwegian Centre for Mental Disorders Research (LAM, TK, AC-P, LTW), K.G. Jebsen Centre for Psychosis Research, Division of Mental Health and Addiction, Oslo University Hospital and Institute of Clinical Medicine, University of Oslo; and Division of Psychiatry (NIL, EH), Diakonhjemmet Hospital, Oslo, Norway; and Department of Pediatrics (AC-P), Stanford University School of Medicine, Stanford, California.

Address correspondence to Luigi A. Maglanoc, M.Sc., Department of Psychology, University of Oslo, P.O. Box 1094 Blindern, 0317 Oslo, Norway; E-mail: luigi.maglanoc@psykologi.uio.no.

Received Apr 4, 2018; revised May 10, 2018; accepted May 21, 2018.

Supplementary material cited in this article is available online at https://doi.org/10.1016/j.bpsc.2018.05.005.

REFERENCES

1. Global Burden of Disease Study 2016 Disease and Injury Incidence and Prevalence Collaborators (2017): Global, regional, and national incidence, prevalence, and years lived with disability for 328 diseases and injuries for 195 countries, 1990–2016: A systematic analysis for the Global Burden of Disease Study 2016. Lancet 390:1211–1259.
2. Friedrich MJ (2017): Depression is the leading cause of disability around the world. JAMA 317:1517.
3. Global Burden of Disease Study 2013 Collaborators (2015): Global, regional, and national incidence, prevalence, and years lived with disability for 301 acute and chronic diseases and injuries in 188 countries, 1990–2013: A systematic analysis for the Global Burden of Disease Study 2013. Lancet 386:743–800.
4. Drevets WC, Savitz J, Trimble M (2008): The subgenual anterior cingulate cortex in mood disorders. CNS Spectr 13:663–681.
5. Insel TR, Landis SC (2013): Twenty-five years of progress: The view from NIMH and NINDS. Neuron 80:561–567.
6. Müller VI, Cieslik EC, Serbanescu I, Laird AR, Fox PT, Eickhoff SB (2017): Altered brain activity in unipolar depression revisited: Meta-analyses of neuroimaging studies. JAMA Psychiatry 74:47–55.
7. Fried EI, Nesse RM (2015): Depression is not a consistent syndrome: An investigation of unique symptom patterns in the STAR*D study. J Affect Disord 172:96–102.
8. Lamers F, van Oppen P, Comijs HC, Smit JH, Spinhoven P, van Balkom AJ, *et al.* (2011): Comorbidity patterns of anxiety and depressive disorders in a large cohort study: The Netherlands Study of Depression and Anxiety (NESDA). J Clin Psychiatry 72:341–348.
9. Mulders PC, van Eijndhoven PF, Schene AH, Beckmann CF, Tendolkar I (2015): Resting-state functional connectivity in major depressive disorder: A review. Neurosci Biobehav Rev 56:330–344.
10. van den Heuvel MP, Sporns O (2013): Network hubs in the human brain. Trends Cogn Sci 17:689–696.
11. Marchetti I, Koster EHW, Sonuga-Barke EJ, De Raedt R (2012): The default mode network and recurrent depression: A neurobiological model of cognitive risk factors. Neuropsychol Rev 22:229–251.
12. Hutchison RM, Womelsdorf T, Allen EA, Bandettini PA, Calhoun VD, Corbetta M, *et al.* (2013): Dynamic functional connectivity: Promise, issues, and interpretations. Neuroimage 80:360–378.
13. Bassett DS, Wymbs NF, Porter MA, Mucha PJ, Carlson JM, Grafton ST (2011): Dynamic reconfiguration of human brain networks during learning. Proc Natl Acad Sci U S A 108:7641–7646.
14. Damaraju E, Allen EA, Belger A, Ford JM, McEwen S, Mathalon DH, *et al.* (2014): Dynamic functional connectivity analysis reveals transient states of dysconnectivity in schizophrenia. Neuroimage Clin 5:298–308.
15. Chen Y, Wang W, Zhao X, Sha M, Liu Y, Zhang X, *et al.* (2017): Age-related decline in the variation of dynamic functional connectivity: A resting state analysis. Front Aging Neurosci 9:203.
16. Demirtas M, Tornador C, Falcon C, Lopez-Sola M, Hernandez-Ribas R, Pujol J, *et al.* (2016): Dynamic functional connectivity reveals altered variability in functional connectivity among patients with major depressive disorder. Hum Brain Mapp 37:2918–2930.
17. Bouveyron C, Girard S, Schmid C (2007): High-dimensional data clustering. Comput Stat Data Anal 52:502–519.
18. First MB, Spitzer RL, Gibbons M, Williams JBW (2002): Structured Clinical Interview for DSM-IV-TR Axis I Disorders, Research Version, Patient Edition. (SCID-I/P). New York, NY: Biometrics Research, New York State Psychiatric Institute.
19. Sheehan DV, Lecrubier Y, Sheehan KH, Amorim P, Janavs J, Weiller E, *et al.* (1998): The Mini-International Neuropsychiatric Interview (M.I.N.I.): The development and validation of a structured diagnostic psychiatric interview for DSM-IV and ICD-10. J Clin Psychiatry 59:22–33.
20. Beck AT (1996): Manual for the Beck Depression Inventory-II. San Antonio, TX: Psychological Corporation.
21. Beck AT, Steer RA (1993): Beck Anxiety Inventory Manual. San Antonio, TX: Psychological Corporation.
22. Bergé L, Bouveyron C, Girard S (2012): HDclassif: An R package for model-based clustering and discriminant analysis of high-dimensional data. J Stat Softw 46:1–29.
23. Fraley C, Raftery AE (1999): mclust: Software for model-based cluster analysis. J Classif 16:297–306.
24. Ramey JA (2012): clusteval: Evaluation of clustering algorithms. Available at: https://cran.r-project.org/package=clusteval. Accessed January 16, 2018.
25. Rubinov M, Sporns O (2010): Complex network measures of brain connectivity: Uses and interpretations. Neuroimage 52:1059–1069.
26. Epskamp S, Cramer AOJ, Waldorp LJ, Schmittmann VD, Borsboom D (2012): qgraph: Network visualizations of relationships in psychometric data. J Stat Softw 48.
27. Smith SM, Jenkinson M, Woolrich MW, Beckmann CF, Behrens TE, Johansen-Berg H, *et al.* (2004): Advances in functional and structural MR image analysis and implementation as FSL. Neuroimage 23:S208–S219.
28. Jenkinson M, Bannister P, Brady M, Smith S (2002): Improved optimization for the robust and accurate linear registration and motion correction of brain images. Neuroimage 17:825–841.
29. Salimi-Khorshidi G, Douaud G, Beckmann CF, Glasser MF, Griffanti L, Smith SM (2014): Automatic denoising of functional MRI data: Combining independent component analysis and hierarchical fusion of classifiers. Neuroimage 90:449–468.
30. Griffanti L, Salimi-Khorshidi G, Beckmann CF, Auerbach EJ, Douaud G, Sexton CE, *et al.* (2014): ICA-based artefact removal and accelerated fMRI acquisition for improved resting state network imaging. Neuroimage 95:232–247.

31. Kaufmann T, Alnæs D, Doan NT, Brandt CL, Andreassen OA, Westlye LT (2017): Delayed stabilization and individualization in connectome development are related to psychiatric disorders. Nat Neurosci 20:513–515.
32. Skåtun KC, Kaufmann T, Tønnesen S, Biele G, Melle I, Agartz I, *et al.* (2016): Global brain connectivity alterations in patients with schizophrenia and bipolar spectrum disorders. J Psychiatry Neurosci 41:331–341.
33. Roalf DR, Quarmley M, Elliott MA, Satterthwaite TD, Vandekar SN, Ruparel K, *et al.* (2016): The impact of quality assurance assessment on diffusion tensor imaging outcomes in a large-scale population-based cohort. Neuroimage 125:903–919.
34. Córdova-Palomera A, Kaufmann T, Persson K, Alnæs D, Doan NT, Moberget T, *et al.* (2017): Disrupted global metastability and static and dynamic brain connectivity across individuals in the Alzheimer's disease continuum. Sci Rep 7:40268.
35. Fischl B, Salat DH, Busa E, Albert M, Dieterich M, Haselgrove C, *et al.* (2002): Whole brain segmentation: Automated labeling of neuroanatomical structures in the human brain. Neuron 33:341–355.
36. Greve DN, Fischl B (2009): Accurate and robust brain image alignment using boundary based registration. Neuroimage 48:63–72.
37. Kaufmann T, Skåtun KC, Alnæs D, Doan NT, Duff EP, Tønnesen S, *et al.* (2015): Disintegration of sensorimotor brain networks in schizophrenia. Schizophr Bull 41:1326–1335.
38. Abou Elseoud A, Littow H, Remes J, Starck T, Nikkinen J, Nissilä J, *et al.* (2011): Group-ICA model order highlights patterns of functional brain connectivity. Front Syst Neurosci 5:37.
39. Filippini N, Macintosh BJ, Hough MG, Goodwin GM, Frisoni GB, Smith SM, *et al.* (2009): Distinct patterns of brain activity in young carriers of the APOE-epsilon4 allele. Proc Natl Acad Sci U S A 106:7209–7214.
40. Kelly REJ, Alexopoulos GS, Wang Z, Gunning FM, Murphy CF, Morimoto SS, *et al.* (2010): Visual inspection of independent components: Defining a procedure for artifact removal from fMRI data. J Neurosci Methods 189:233–245.
41. Friedman J, Tibshirani R (2008): Sparse inverse covariance estimation with the graphical lasso. Biostatistics 9:432–441.
42. Ledoit O, Wolf M (2003): Improved estimation of the covariance matrix of stock returns with an application to portfolio selection. J Empir Finance 10:603–621.
43. Glerean E, Salimi J, Lahnakoski JM, Jääskeläinen IP, Sams M (2012): Functional magnetic resonance imaging phase synchronization as a measure of dynamic functional connectivity. Brain Connect 2:91–101.
44. Deco G, Kringelbach ML (2016): Metastability and coherence: Extending the communication through coherence hypothesis using a whole-brain computational perspective. Trends Neurosci 39:125–135.
45. Shanahan M (2010): Metastable chimera states in community-structured oscillator networks. Chaos 20:13108.
46. Cabral J, Hugues E, Sporns O, Deco G (2011): Role of local network oscillations in resting-state functional connectivity. Neuroimage 57:130–139.
47. Hellyer PJ, Scott G, Shanahan M, Sharp DJ, Leech R (2015): Cognitive flexibility through metastable neural dynamics is disrupted by damage to the structural connectome. J Neurosci 35:9050–9063.
48. Kahana MJ (2006): The cognitive correlates of human brain oscillations. J Neurosci 26:1669–1672.
49. Naik S, Banerjee A, Bapi RS, Deco G, Roy D (2017): Metastability in senescence. Trends Cogn Sci 21:509–521.
50. Váša F, Shanahan M, Hellyer PJ, Scott G, Cabral J, Leech R (2015): Effects of lesions on synchrony and metastability in cortical networks. Neuroimage 118:456–467.
51. Fries P (2005): A mechanism for cognitive dynamics: Neuronal communication through neuronal coherence. Trends Cogn Sci 9:474–480.
52. Zalesky A, Fornito A, Bullmore ET (2010): Network-based statistic: Identifying differences in brain networks. Neuroimage 53:1197–1207.
53. R Core Team (2017): R: A Language and Environment for Statistical Computing. Vienna, Austria: R Foundation for Statistical Computing.
54. Lamers F, de Jonge P, Nolen WA, Smit JH, Zitman FG, Beekman AT, Penninx BW (2010): Identifying depressive subtypes in a large cohort study: Results from the Netherlands Study of Depression and Anxiety (NESDA). J Clin Psychiatry 71:1582–1589.
55. Rodgers S, Ajdacic-Gross V, Müller M, Hengartner MP, Grosse Holtforth M, Angst J, Rössler W (2014): The role of sex on stability and change of depression symptom subtypes over 20 years: A latent transition analysis. Eur Arch Psychiatry Clin Neurosci 264:577–588.
56. Alexandrino-Silva C, Wang YP, Carmen Viana M, Bulhões RS, Martins SS, Andrade LH (2013): Gender differences in symptomatic profiles of depression: Results from the São Paulo Megacity Mental Health Survey. J Affect Disord 147:355–364.
57. American Psychiatric Association (2013): Diagnostic and Statistical Manual of Mental Disorders, 5th ed. Washington, DC: American Psychiatric Publishing.
58. van Loo HM, de Jonge P, Romeijn JW, Kessler RC, Schoevers RA (2012): Data-driven subtypes of major depressive disorder: A systematic review. BMC Med 10:156.
59. van Borkulo C, Boschloo L, Borsboom D, Penninx B, Waldorp L, Schoevers R (2016): Association of symptom network structure with the course of longitudinal depression. JAMA Psychiatry 73:412.
60. Fried EI, Nesse RM, Guille C, Sen S (2015): The differential influence of life stress on individual symptoms of depression. Acta Psychiatr Scand 131:465–471.
61. Keller MC, Neale MC, Kendler KS (2007): Association of different adverse life events with distinct patterns of depressive symptoms. Am J Psychiatry 164:1521–1529.
62. Geoffroy PA, Hoertel N, Etain B, Bellivier F, Delorme R, Limosin F, Peyre H (2018): Insomnia and hypersomnia in major depressive episode: Prevalence, sociodemographic characteristics and psychiatric comorbidity in a population-based study. J Affect Disord 226:132–141.
63. McKinnon AC, Hickie IB, Scott J, Duffy SL, Norrie L, Terpening Z, *et al.* (2017): Current sleep disturbance in older people with a lifetime history of depression is associated with increased connectivity in the Default Mode Network. J Affect Disord 229:85–94.
64. Braun U, Schäfer A, Walter H, Erk S, Romanczuk-Seiferth N, Haddad L, *et al.* (2015): Dynamic reconfiguration of frontal brain networks during executive cognition in humans. Proc Natl Acad Sci U S A 112:11678–11683.
65. Rusnáková S, Daniel P, Chládek J, Jurák P, Rektor I (2011): The executive functions in frontal and temporal lobes: A flanker task intracerebral recording study. J Clin Neurophysiol 28:30–35.
66. Menon V (2011): Large-scale brain networks and psychopathology: A unifying triple network model. Trends Cogn Sci 15:483–506.
67. Perrin JS, Merz S, Bennett DM, Currie J, Steele DJ, Reid IC, Schwarzbauer C (2012): Electroconvulsive therapy reduces frontal cortical connectivity in severe depressive disorder. Proc Natl Acad Sci U S A 109:5464–5468.
68. Sheline YI, Barch DM, Price JL, Rundle MM, Vaishnavi SN, Snyder AZ, *et al.* (2009): The default mode network and self-referential processes in depression. Proc Natl Acad Sci U S A 106:1942–1947.
69. Liu CH, Ma X, Yuan Z, Song LP, Jing B, Lu HY, *et al.* (2017): Decreased resting-state activity in the precuneus is associated with depressive episodes in recurrent depression. J Clin Psychiatry 78:e372–e382.
70. Berman MG, Peltier S, Nee DE, Kross E, Deldin PJ, Jonides J (2011): Depression, rumination and the default network. Soc Cogn Affect Neurosci 6:548–555.
71. Xu LY, Xu FC, Liu C, Ji YF, Wu JM, Wang Y, *et al.* (2017): Relationship between cerebellar structure and emotional memory in depression. Brain Behav 7:e00738.
72. Webb CA, Weber M, Mundy EA, Killgore WD (2014): Reduced pink matter volume in the anterior cingulate, orbitofrontal cortex and thalamus as a function of mild depressive symptoms: A voxel-based morphometric analysis. Psychol Med 44:2833–2843.
73. Drysdale AT, Grosenick L, Downar J, Dunlop K, Mansouri F, Meng Y, *et al.* (2017): Resting-state connectivity biomarkers define neurophysiological subtypes of depression. Nat Med 23:28–38.

74. Price RB, Gates K, Kraynak TE, Thase ME, Siegle GJ (2017): Data-driven subgroups in depression derived from directed functional connectivity paths at rest. Neuropsychopharmacology 42:2623–2632.
75. Kendler KS, Aggen SH, Flint J, Borsboom D, Fried EI (2018): The centrality of DSM and non-DSM depressive symptoms in Han Chinese women with major depression. J Affect Disord 227:739–744.
76. Fried EI, Epskamp S, Nesse RM, Tuerlinckx F, Borsboom D (2016): What are "good" depression symptoms? Comparing the centrality of DSM and non-DSM symptoms of depression in a network analysis. J Affect Disord 189:314–320.
77. Fried EI (2017): The 52 symptoms of major depression: Lack of content overlap among seven common depression scales. J Affect Disord 208:191–197.
78. Kaiser RH, Whitfield-Gabrieli S, Dillon DG, Goer F, Beltzer M, Minkel J, *et al.* (2015): Dynamic resting-state functional connectivity in major depression. Neuropsychopharmacology 41:1–9.
79. Wise T, Marwood L, Perkins AM, Herane-Vives A, Joules R, Lythgoe DJ, *et al.* (2017): Instability of default mode network connectivity in major depression: A two-sample confirmation study. Transl Psychiatry 7:e1105.
80. Smith SM, Miller KL, Salimi-Khorshidi G, Webster M, Beckmann CF, Nichols TE, *et al.* (2011): Network modeling methods for FMRI. Neuroimage 54:879–891.
81. Yu Q, Du Y, Chen J, He H, Sui J, Pearlson G, Calhoun VD (2017): Comparing brain graphs in which nodes are regions of interest or independent components: A simulation study. J Neurosci Methods 291:61–68.
82. Hindriks R, Adhikari MH, Murayama Y, Ganzetti M, Mantini D, Logothetis NK, Deco G (2016): Can sliding-window correlations reveal dynamic functional connectivity in resting-state fMRI? Neuroimage 127:242–256.
83. Power JD, Barnes KA, Snyder AZ, Schlaggar BL, Petersen SE (2012): Spurious but systematic correlations in functional connectivity MRI networks arise from subject motion. Neuroimage 59: 2142–2154.
84. Yan CG, Cheung B, Kelly C, Colcombe S, Craddock RC, Di Martino A, *et al.* (2013): A comprehensive assessment of regional variation in the impact of head micromovements on functional connectomics. Neuroimage 76:183–201.